CALCULATION

of the

BRIGHTNESS OF LIGHT

IN THE CASE OF
ANISOTROPIC SCATTERING

(PART 2)

[Transactions (Trudy) of the Institute of Atmospheric Physics No. 3]

CALCULATION of the

BRIGHTNESS OF LIGHT

IN THE CASE OF ANISOTROPIC SCATTERING

(Part 2)

V. S. Atroshenko, E. M. Feigelson, K. S. Glazova, and M. S. Malkevich

AUTHORIZED TRANSLATION FROM THE RUSSIAN



CONSULTANTS BUREAU, NEW YORK 1963

Original Russian text published by the Academy of Sciences USSR Press in Moscow in 1962.

Library of Congress Catalog Card Number 60-8720

COPYRIGHT 1963 BY CONSULTANTS BUREAU ENTERPRISES, INC. 227 West 17th Street, New York 11, New York

ALL RIGHTS RESERVED.

NO PART OF THIS BOOK MAY BE REPRODUCED IN ANY FORM WITHOUT THE WRITTEN PERMISSION OF THE PUBLISHER.

PRINTED IN THE UNITED STATES

РАСЧЕТ ЯРКОСТИ СВЕТА В АТМОСФЕРЕ ПРИ АНИЗОТРОПНОМ РАССЕЯНИИ

RASCHET YARKOSTI SVETA V ATMOSFERE PRI ANIZOTROPNOM RASSEYANII

CALCULATION OF THE BRIGHTNESS OF LIGHT IN THE CASE OF ANISOTROPIC SCATTERING

TABLE OF CONTENTS

INTRODUCTION	1
CHAPTER I. SUPPLEMENTARY CALCULATIONS	3
 Basic Relations and Notation The Supplementary Calculations Intensity of Scattered Light for a Finite Surface Albedo Multiple Scattering Relation Between Optical Thickness and Height 	3 8 8 13 16
CHAPTER II. SKY BRIGHTNESS AT 5 TO 30 KM	18
Introduction. § 1. Development of the Sky Brightness in the Upper Atmosphere § 2. Distribution of Brightness with Height	18 21 28 40 45
CHAPTER III. EMERGENCE OF RADIATION FROM THE ATMOSPHERE	51
Introduction. \$ 1. Intensity of the Emergent Radiation. \$ 2. Brightness Coefficient of the Atmosphere \$ 3. Flux of the Emergent Radiation. \$ 4. Albedo of the Earth—Atmosphere System	51 52 56 57 58
CHAPTER IV. DAYLIGHT VISIBILITY FROM THE SURFACE OF OBJECTS IN THE AIR	64
Introduction § 1. Method of Calculation	64 65 70
CHAPTER V. APPROXIMATE METHODS FOR SOLVING TRANSFER EQUATIONS	78
Introduction § 1. The Flux Equation § 2. Variability of the Coefficients in the Flux Equation § 3. An Approximate Method for Determining the Coefficients	78 78 80
of Eqs. (5.1)	85 90 94

CONTENTS (continued)

APPE	NDIX.	EXPLAN	ATION OF THE TABLES	111
	TABLE	E I.	Intensity of Scattered Radiation	114
	TABLE	II.	Ascending Radiation, $q \neq 0 \dots \dots \dots$	134
	TABLE	III.	Descending Radiation, q ≠ 0	144
	TABLE	IV.	Ratio of Ascending to Singly Scattered Radiation	154
	TABLE	V.	Ratio of Descending to Singly Scattered Radiation	166
	TABLE	VI.	Fraction of Brightness Above the Surface Due	
			to Multiple Scattering	177
	TABLE	VII.	Brightness of the Sky, $q = 0.2$	178
	TABLE	VIII1.	Spectral Sky Brightness, q=0	179
	TABLE	VIII ₂ .	Spectral Sky Brightness, Grass Cover	181
	TABLE	VIII ₃ .	Spectral Sky Brightness, Snow Cover	184
	TABLE	IX.	The Solar Constant	187
	TABLE	X.	Limiting Magnitudes	187
	TABLE	XI.	Emergent Radiation Intensity	188
	TABLE	XII.	Brightness Coefficients	190
	TABLE	XIII.	Emergent Radiation Flux	191
	TABLE	XIV.	Combined Albedo, Earth—Atmosphere System	191
	TABLE	XV_1 .	Brightness of Object in Shadow	192
	TABLE	XV ₂ .	Brightness of Sunlit Object	196
	TABLE	XVI1.	Brightness Contrast, Object in Shadow. Albedo = 1	200
	TABLE	XVI2.	Brightness Contrast, Object in Shadow. Albedo = 0.1	204
	TABLE	XVII1.	Brightness Contrast, Sunlit Object. Albedo = 1	208
	TABLE	XVII ₂ .	Brightness Contrast, Sunlit Object. Albedo = 0.1	212
	TABLE	XVIII.	Coefficients of Flux Equations	216
	TABLE	XIX.	Mean Coefficients of Flux Equations	224
	TABLE	XX.	Comparison of Approximate and Exact Values of Flux	226

INTRODUCTION

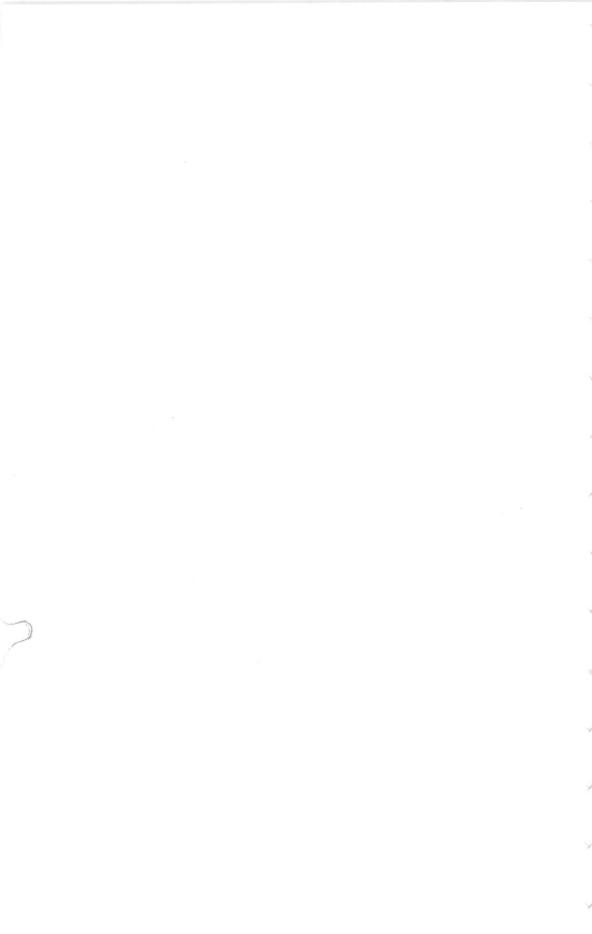
The present volume forms the second part of an investigation of the intensity of scattered light in the anisotropically scattering atmosphere. The first part was published in 1958 as No. 1 of the Transactions (Trudy) of the Institute of Atmospheric Physics. Auxiliary tables are provided here for the intensity of the scattered light, and further analyses are made of the various factors responsible for the scattered radiation. The behavior of the brightness of the sky in the upper atmosphere (up to 30 km), and the radiation emerging from the upper atmosphere into outer space, is examined. Calculations are made for the brightness of objects in the atmosphere illuminated by direct and scattered sunlight. These investigations constitute the first portion of the volume (Chapters I-IV).

The second portion (Chapter V) provides an evaluation and improvement of approximate methods for solving transfer equations. Thus, the present volume attempts to apply the results of Part 1 to the solution of such practical problems as range of visibility and aerial photography, and to the development of techniques in the mathematical theory of radiative transfer.

Chapter I was written by K. S. Glazova, M. S. Malkevich, and E. M. Feigel'son; Chapter II by Feigel'son; Chapter III by Malkevich; Chapter IV by V. S. Atroshenko and Feigel'son; and Chapter V by Atroshenko and Malkevich.

É. Kim and L. Tomashova, students at Moscow University, have assisted with the work on Chapters II and III, respectively. The authors wish to express their gratitude for this assistance.

The authors are also indebted to M. A. Kuznetsova, E. P. Petrova, Z. N. Tarasenkova, and L. A. Kazenova, research assistants at the Institute of Atmospheric Physics, USSR Academy of Sciences, for performing the extensive computations.



CHAPTER I

SUPPLEMENTARY CALCULATIONS

§ 1. Basic Relations and Notation

The research described in this volume is based on a theory developed in Part 1 of the monograph [1]. We review here the principal concepts, relations, and notation introduced in Part 1.

As in Part 1, our results represent numerical solutions of radiative-transfer equations of the form

$$\cos \theta \frac{\partial I_{\lambda}(\tau, r)}{\partial \tau} = \frac{1}{4\pi} \int \overline{I}_{\lambda}(\tau, r') \gamma_{\lambda}(\tau, r, r') d\omega' - \overline{I}_{\lambda}(\tau, r) + \frac{S_{\lambda}}{4} e^{-(\tau^* - \tau) \sec \zeta} \gamma_{\lambda}(\tau, r_{\odot}, r).$$
(1.1)

Equation (1.1) describes the process of radiative transfer in a plane-parallel medium, with a parallel beam of solar radiation incident upon the upper boundary of the medium. Only the scattering process occurs within the medium.

The following notation appears in Eq. (1.1): $\overline{I}_{\lambda}(\tau,r)$ is the intensity of the scattered radiation. The wavelength-dependent optical thickness τ of the atmosphere is given by the formula

$$\tau = \int_{0}^{z} \sigma_{\lambda}(y) \, dy, \tag{1.2}$$

where $\sigma(y)$ is the scattering coefficient. The optical thickness $\tau*$ of the entire atmosphere is computed from Eq. (1.2), with $z=\infty$. In Part 2 we shall also encounter the quantity τ ', the optical depth measured from the upper boundary of the atmosphere. Evidently

$$\tau' = \tau^* - \tau = \int_{z}^{\infty} \sigma(\zeta) d\zeta. \tag{1.3}$$

In Eq. (1.1), the symbol r connotes the direction of propagation of the radiation; it can be specified by the polar angle θ and the azimuth ψ .

The relative scattering function $\gamma_{\lambda}(au, r, r')$ satisfies the normalization condition

$$\frac{1}{4\pi} \int \gamma(\tau, r, r') d\omega' = 1. \tag{1.4}$$

We shall denote by φ the angle between the directions r' of the incident ray and r of the scattered ray; this is the scattering angle. We have the relation

$$\cos \varphi = \cos \theta \cos \theta' + \sin \theta \sin \theta' \cos (\psi - \psi'). \tag{1.5}$$

The solar constant for wavelength λ is denoted by πS_{λ} ; r_{\odot} is the direction of propagation of sunlight;

$$\psi_{\odot}=0;\ \theta_{0}=\pi-\xi;$$

and & is the zenith distance of the sun.

The integration in Eq. (1.1) extends over a sphere of unit radius with the element $d\omega'$ of solid angle given by

$$d\omega' = \sin\theta d\theta d\psi$$
.

All the calculations in Part 1 refer to relative intensities $I(\tau, r)$, where

$$I(\tau, r) = \frac{2}{S} \overline{I}(\tau, r).$$

We shall here be concerned mainly with $I(\tau, r)$ and the other relative quantities corresponding to it.

It is convenient to consider separately the radiation propagated in the ascending and descending directions. Measuring θ from the zenith direction, we shall use the following notation for the upward and downward radiation, respectively:

$$I_{\lambda}(\tau, r) = \begin{cases} I_{\lambda}^{(1)}(\tau, r) & 0 \leqslant \theta \leqslant \frac{\pi}{2} \\ & 0 \leqslant \psi \leqslant 2\pi \end{cases}$$

$$I_{\lambda}(\tau, r) = \begin{cases} I_{\lambda}^{(2)}(\tau, r) & \frac{\pi}{2} \leqslant \theta \leqslant \pi \\ & 0 \leqslant \psi \leqslant 2\pi. \end{cases}$$

$$(1.6)$$

The corresponding scattering functions are

$$\gamma_{1,1,\lambda}(\tau, r, r') = \begin{cases}
\gamma_{1,1,\lambda}(\tau, r, r') & 0 \leqslant \theta \leqslant \frac{\pi}{2} \\
0 \leqslant \theta' \leqslant \frac{\pi}{2}
\end{cases}$$

$$\gamma_{1,2,\lambda}(\tau, r, r') = \begin{cases}
\gamma_{1,2,\lambda}(\tau, r, r') & \frac{\pi}{2} \leqslant \theta \leqslant \pi \\
0 \leqslant \theta' \leqslant \frac{\pi}{2}
\end{cases}$$

$$\gamma_{2,1,\lambda}(\tau, r, r') = \begin{cases}
\frac{\pi}{2} \leqslant \theta \leqslant \pi \\
0 \leqslant \theta' \leqslant \frac{\pi}{2}
\end{cases}$$

$$\gamma_{2,2,\lambda}(\tau, r, r') = \frac{\pi}{2} \leqslant \theta \leqslant \pi$$

$$\gamma_{2,2,\lambda}(\tau, r, r') = \frac{\pi}{2} \leqslant \theta \leqslant \pi$$

$$\frac{\pi}{2} \leqslant \theta \leqslant \pi$$

$$\frac{\pi}{2} \leqslant \theta \leqslant \pi$$

The following system now replaces Eq. (1.1):

$$\cos\theta \frac{\partial I_{\lambda}^{(1)}}{\partial \tau} = K_{\lambda}^{(1)}(\tau, r) - I_{\lambda}^{(1)}(\tau, r) + \frac{1}{2}e^{-(\tau^* - \tau)\sec\xi} \times \times \gamma_{1,2,\lambda}(\tau, r, r'),$$

$$-\cos\theta \frac{\partial I_{\lambda}^{(2)}}{\partial \tau} = K_{\lambda}^{(2)}(\tau, r) - I_{\lambda}^{(2)}(\tau, r) + \frac{1}{2}e^{-(\tau^* - \tau)\sec\xi} \times \times \gamma_{2,2,\lambda}(\tau, r, r'),$$

$$(1.8)$$

where

$$K_{\lambda}^{(1)}(\tau, r) = \frac{1}{4\pi} \int_{+}^{1} I_{\lambda}^{(1)} \gamma_{1,1,\lambda} d\omega' + \frac{1}{4\pi} \int_{+}^{1} I_{\lambda}^{(2)} \cdot \gamma_{1,2,\lambda} d\omega',$$

$$K_{\lambda}^{(2)}(\tau, r) = \frac{1}{4\pi} \int_{+}^{1} I_{\lambda}^{(1)} \gamma_{2,1,\lambda} d\omega' + \frac{1}{4\pi} \int_{+}^{1} I_{\lambda}^{(2)} \cdot \gamma_{2,2,\lambda} d\omega'.$$

$$(1.9)$$

Here the integration with respect to solid angle extends over a hemisphere only

$$\int_{+}^{\infty} f(r) d\omega = \int_{0}^{2\pi} \int_{0}^{\frac{\pi}{2}} f(\theta, \psi) \sin \theta d\theta d\psi.$$

Equations (1.8) are to be solved under the boundary conditions

$$I_{\lambda}^{(2)}(\tau^*, r) = 0 \quad \text{or} \quad \frac{\pi}{2} \leqslant \theta \leqslant \pi, \ 0 \leqslant \psi \leqslant 2\pi,$$
 (1.10)

$$F_{\lambda}^{(1)}(0) = q_{\lambda} \widetilde{F}_{\lambda}^{(2)}(0),$$
 (1.11)

where

$$\frac{S_{\lambda}}{2}\widetilde{F}_{\lambda}^{(2)}(0) = \pi S_{\lambda} e^{-\tau^* \sec \zeta} \cos \zeta + \frac{S_{\lambda}}{2} F_{\lambda}^{(2)}(0), \tag{1.12}$$

 q_λ is the albedo of the earth's surface, and $F_\lambda^{(i)}(\tau)$ is the flux of scattered radiation, defined by the relation

$$F_{\lambda}^{(i)}(\tau) = \int_{+}^{\cdot} I_{\lambda}^{(i)}(\tau, r) \cos \theta d\omega. \tag{1.13}$$

The first term on the right-hand side of Eq. (1.12) represents the flux of direct sunlight at the surface.

By developing the scattering function as a sum of Legendre polynomials,

$$\gamma_{\lambda}(\tau, r, r') = \sum_{j=1}^{N} c_{j,\lambda}(\tau) P_{j} [\cos(r, r')],$$
 (1.14)

we can obtain the solution in the form of a trigonometric series

$$I_{\lambda}^{(i)}(\tau, r) = \frac{1}{2} A_{0,\lambda}^{(i)}(\tau, \theta) + \sum_{k=1}^{N} A_{k,\lambda}^{(i)}(\tau, \theta) \cos k\psi.$$
 (1.15)

The system (1.8) then transforms into a system of 2N equations in the unknowns $A_{k,\lambda}^{(i)}(\tau,\theta)$ (i = 1, 2; k = 1, . . . , N) of the form¹

$$\cos\theta \frac{\partial A_{k}^{(1)}}{\partial \tau} = \frac{1}{2} \int_{0}^{\frac{\pi}{2}} A_{k}^{(1)}(\tau, \theta') \sum_{i=k}^{N} \frac{2}{2i+1} c_{i}(\tau) \overline{P}_{i}^{(k)}(\cos\theta) \times$$

$$\times \overline{P}_{i}^{(k)}(\cos\theta') \sin\theta' d\theta' + \frac{1}{2} \int_{0}^{\frac{\pi}{2}} A_{k}^{(2)}(\tau, \theta') \sum_{i=k}^{N} \frac{2}{2i+1} (-1)^{i-k} \times$$

$$\times c_{i}(\tau) \overline{P}_{i}^{k}(\cos\theta) \overline{P}_{i}^{k}(\cos\theta) \sin\theta' d\theta' - A_{k}^{(1)}(\tau, \theta) +$$

$$+ \frac{1}{2} e^{-(\tau^* - \tau)\sec \zeta} \sum_{i=k}^{N} (-1)^i \frac{2}{2i+1} c_i(\tau) \overline{P}_i^k(\cos \theta') \overline{P}_i^{(k)}(\cos \zeta); \quad k = 1, \dots, N. \quad (1.16)$$

Here the $\overline{\textbf{P}}_i^{(k)}$ are the normalized associated Legendre polynomials. Analogous equations hold for the quantities $A_k^{(2)}$.

Upon solving the system of equations (1.16) by successive approximations, we obtain tables for the intensities $I^{(1)}(\tau,r)$ and $I^{(2)}(\tau,r)$ of the scattered light for the case q=0. As a zero-order approximation, we have taken the corresponding intensities $i^{(1)}(\tau,r)$ and $i^{(2)}(\tau,r)$ of singly scattered light. The intensity $I^{(1)}_q(\tau,r)$ for $q\neq 0$ is then determined from the formula

$$I_q^{(i)}(\tau, r) = I^{(i)}(\tau, r) + C^* B^{(i)}(\tau, \theta),$$
 (1.17)

where the factor C* depends only on q, ζ , and $\gamma(\tau, r, r')$. The functions $B^{(i)}(\tau, \theta)$ are determined from equations differing from Eqs. (1.8) only in the form of the free term. Tables of the quantities C* and $B^{(i)}(\tau, \theta)$ have been given in Part 1.

The descending singly scattered radiation naturally will not depend on q. We denote by $i_q^{(i)}(\tau,\,r)$ the ascending singly scattered radiation for nonvanishing q. A method for determining it will be described presently.

In many cases, it is useful to pass from the integrodifferential equations (1.8) to equivalent integral equations of the form

$$I^{(1)}(\tau, r) = I^{(1)}(0, r) e^{-\tau \sec \theta} + \sec \theta \int_{0}^{\tau} e^{-(\tau - t)\sec \theta} K^{(1)}(t, r) dt + \frac{1}{2} \sec \theta \int_{0}^{\tau} e^{-(\tau - t)\sec \theta} e^{-(\tau^* - t)\sec \xi} \gamma_{21} dt,$$

$$I^{(2)}(\tau, r) = \sec \theta \int_{\tau}^{\tau^*} e^{-(t - \tau)\sec \theta} K^{(2)}(t, r) dt + \frac{1}{2} \sec \theta \int_{\tau}^{\tau^*} e^{-(t - \tau)\sec \theta} e^{-(\tau^* - t)\sec \xi} \gamma_{22} dt. \tag{1.18}$$

We henceforth omit the wavelength designation from all symbols.

One advantage is that the method of successive approximations applies to integral equations of the type (1.18) for determining $A_k^{(i)}(\tau, \theta)$.

In the theory of visibility, aerial photography, and other applications, we often encounter the concept of atmospheric haze, the scattered light sent into a given direction by a particular layer of the atmosphere. Evidently, the brightness $I_q^{(i)}(\tau_1, \tau_2, r)$ of the haze $(\tau_1$ and τ_2 are the optical thicknesses to the lower and upper boundaries of the layer) is given by the relations

$$I_{q}^{(1)}(\tau_{1}, \tau_{2}, r) = I^{(1)}(0, r) e^{-\sec\theta \tau_{2}} + \sec \theta \int_{\tau_{1}}^{\tau_{2}} e^{-\sec\theta(\tau - t)} K^{(1)}(t, r) dt +$$

$$+ \sec \theta \int_{\tau_{1}}^{\tau_{2}} e^{-\sec\theta(\tau_{2} - t)} e^{-\sec\xi(\tau^{*} - t)} \gamma_{21}(t, r_{\odot}, r) dt, \qquad (1.19)$$

$$I_{q}^{(2)}(\tau_{1}, \tau_{2}, r) = \sec \theta \int_{\tau_{1}}^{\tau_{2}} e^{-\sec \theta (t - \tau_{1})} K^{(2)}(t, r) dt +$$

$$+ \sec \theta \int_{\tau_{1}}^{\tau_{2}} e^{-\sec \theta (t - \tau_{1})} e^{-\sec \zeta(\tau^{*} - t)} \gamma_{22}(t, r_{\odot}, r) dt.$$

$$(1.20)$$

Combining with Eqs. (1.18), we obtain the following expressions for the haze intensity in the ascending and descending directions, respectively:

$$I_q^{(1)}(\tau_1, \tau_2, r) = I^{(1)}(\tau_2, r) - I^{(1)}(\tau_1, r) e^{-\sec\theta(\tau_2 - \tau_1)},$$
 (1.21)

$$I_q^{(2)}(\tau_1, \tau_2, r) = I^{(2)}(\tau_1, r) - I^{(2)}(\tau_2, r) e^{-\sec\theta(\tau_2 - \tau_1)}$$
 (1.22)

In Part 1, the atmosphere was divided into two layers for the computations of $I^{(i)}(\tau,r)$

$$0\leqslant \tau\leqslant\frac{3}{4}\tau\text{* and }\frac{3}{4}\tau^*\leqslant\tau\leqslant\tau\text{*}.$$

All calculations used the same scattering function in the atmospheric layer $(3/4)\tau * \le \tau \le \tau *$. In the lower portion of the atmosphere, $0 \le \tau \le (3/4)\tau *$, the scattering function was allowed to vary.

Altogether four scattering functions were considered in the lower layer; they are characterized by the "directivity" Γ_1/Γ_2 of the scattered beam, defined as

$$\frac{\Gamma_1}{\Gamma_2} = \frac{\int\limits_0^{\frac{\pi}{2}} \gamma(\varphi) \sin \varphi d\varphi}{\int\limits_{\frac{\pi}{2}}^{\frac{\pi}{2}} \gamma(\varphi) \sin \varphi d\varphi}.$$
 (1.23)

The values of this ratio, which measures the extent to which the scattering function is "drawn out," were as follows for the functions used:

Function number I V VI VII VIII Ratio
$$\Gamma_1/\Gamma_2$$
 1.3 1.8 2.5 4.7 8.4

Here scattering function I is that used for the upper layer of the atmosphere. Scattering functions will always be designated by Roman numerals.

We may finally point out that the brightness of the sky is the intensity $I^{(2)}(\tau, r)$ of the descending scattered radiation. We shall retain this notation for the brightness, but shall also use the customary notation $B(\tau, r)$.

§ 2. The Supplementary Calculations

When solving certain problems in applied atmospheric optics, we often need to know the values of the radiant intensity, $I^{(1)}(\tau, r)$ and $I^{(2)}(\tau, r)$, calculated for the case of a highly transparent atmosphere (small τ^*). For this purpose, we shall take $\tau^*=0.1$, and use the two scattering functions V and VI to find the values of $I^{(1)}(\tau, r)$ and $I^{(2)}(\tau, r)$, for the ζ adopted in Paper 1. These quantities have been computed on the basis of the previous model atmosphere and the previous method. Since τ^* is small, we have restricted ourselves to the first approximation in computing the coefficients of the series in Eq. (1.15) by the successive-approximation procedure (see Paper 1). The results for this case are presented in Table I of the Appendix to this volume. To have a more complete series of optical thickness, ranging from a transparent ($\tau^*=0.1$) to a turbid atmosphere ($\tau^*=0.4$), we have also included in Table I the case $\tau^*=0.3$, with functions V and VI. The notation and format of Table I correspond exactly to that used in Table I of Part 1, which contains the cases $\tau^*=0.2$, 0.4, 0.6, 0.8; and all quantities are given in the same relative units (that is, they must be multiplied by the factor S/2).

§ 3. Intensity of Scattered Light for a Finite Surface Albedo

Tables of the quantities $I^{(i)}(\tau, r)$, C^* , and $B^{(i)}(\tau, \theta)$ are presented in Part 1, and by using them one can immediately compute from Eq. (1.17) the intensity $I_{(i)}^{(i)}(\tau, \theta, \psi)$ of scattered light for arbitrary albedo q.

Nevertheless, we have found it useful to compile explicit tables of $I_q^{(i)}(\tau, r)$ for q = 0.2, 0.4, and 0.8, since an inspection of these tables leads to a number of conclusions about the effect of the albedo on the scattered radiation, supplementing the conclusions mentioned in Part 1.

The quantities $I_q^{(1)}(\tau,\,r)$ and $I_q^{(2)}(\tau,\,r)$ appear,respectively, in Tables II and III of the Appendix.

In addition to the values of I_q , all the tables also contain the derivatives $\Delta(i) = C * B(i)(\tau, \theta)$ [see Eq. (1.17)], namely, the corrections to the intensity because of reflection of direct solar and scattered radiation from the earth's surface.

Consider Table II of the Appendix, particularly the behavior of the correction $\Delta^{(1)} = C * B^{(1)}$. The table shows that:

- 1) $\Delta^{(1)}$ falls off sharply with increasing ζ . The relation (1.12) shows that this behavior arises from the rapid decrease with ζ of the flux of direct sunlight reaching the earth.
- 2) $\Delta^{(1)}$ falls off slowly with increasing τ, τ^* , and θ . In all these cases, the decrease is due to the greater attenuation of the direct sunlight reaching the earth [see Eq. (1.12)], and of the radiation reflected from the surface as it passes through

the atmosphere. The rate of fall in $\Delta^{(1)}$ is mild because scattered radiation on the same trajectory supplements the reflected radiation more fully when τ , $\tau*$, and θ are large

3) $\Delta^{(1)}$ is independent of ψ ; this follows from the assumption in Part 1 that Lambert's law holds at the earth's surface.

TABLE 1

		ζ=30°			ζ=75°	
q	$ \psi = 0^{\circ}; $	$ \theta = 75^{\circ}; $ $ \psi = 0^{\circ} $	$\theta = 75^{\circ};$ $\psi = 180^{\circ}$	$\theta = 0^{\circ};$ $\psi = 0^{\circ}$	$\theta = 75^{\circ};$ $\psi = .0^{\circ}$	$\theta = 75^{\circ};$ $\psi = 180^{\circ}$
			$\tau^* = 0.2$			
()	0	0	0	0	0	0
0.2	87	66	75	64	14	25
().4	94	91	94	85	28	46
0,8	100	108	111	93	47	69
			$\tau^* = 0.6$			
0	0	0	0	0	0	0
0,2	70	52	57	39	7,5	14
0,4	88	84	89	60	15	28
0,8	103	122	128	84	32	54

TABLE 2

	ζ=	=30°	ζ=	=75°
q	ψ=0°	ψ=180°	$\psi{=}{\scriptstyle 0^{\circ}}$	ψ=180°
		$\tau^* = 0.2$		
()	35	40	11	28
0,2	80	89	23	41
0,4	96	100	33	56
0,8	110	110	51	75
		$\tau^* = 0.6$		1
()	40	47	13	27
0,2	74	81	19	37
0,4	95	100	25	45
0,8	118	125	38	65

If we now observe that $I^{(1)}(\tau,\theta,\psi)$ increases with τ,τ^* , and θ because of a greater contribution of scattering, but decreases with ζ because of the weakening of the sunlight and the greater attenuation along the trajectory, we see that the function $I_q^{(1)}$ would in the first instance vary more slowly with τ,θ,τ^* for $q\neq 0$ than for q=0, and it is only the ζ -dependence that makes the variation as strong as it is. Of the two components of the quantity $I_q^{(1)}$, namely $\Delta^{(1)}$ and $I_q^{(1)}$, the first generally predominates. Only for large ζ and θ simultaneously do we have $I_q^{(1)} > \Delta^{(1)}$. But the component

TABLE 3

		$\tau^* = 0.2$			τ*=0,6		
q	θ=0°; ψ=0°	$\theta = 75^{\circ}; \\ \psi = 0^{\circ}$	$\theta = 75^{\circ}; \\ \psi = 180^{\circ}$	$\theta=0^{\circ}; \ \psi=0^{\circ}$	$\theta = 75^{\circ}; \\ \psi = 0^{\circ}$	$\theta = 75^{\circ};$ $\psi = 180^{\circ}$	
0	61	200	115	53	158	95	
0,2	31	110	63	30	120	68	
0,4	27	78	50	25	95	55	
0,8	25	54	37	21	65	40	

TABLE 4

		ζ=30°		ζ=75°			
q	$ \theta = 0^{\circ}; $ $ \psi = 0^{\circ} $	$ \theta = 75^{\circ}; $ $ \psi = 0^{\circ} $	$\theta = 75^{\circ}; \\ \psi = 180^{\circ}$	$ \begin{vmatrix} \theta = 0^{\circ}; \\ \psi = 0^{\circ} \end{vmatrix} $	$\theta = 75^{\circ}; \\ \psi = 0^{\circ}$	$\theta = 75^{\circ}; \\ \psi = 180^{\circ}$	
0	49	55	54	55	70	70	
0,2	90	83	83	92	75	80	
0,4	99	98	99	105	81	90	
0,8	100	109	111	119	90	104	

TABLE 5

	ζ=	=30°	ζ=	-75°
q	τ*=0,2	$\tau^* = 0.6$	τ*=0,2	τ*=0,6
0	85	72	50	50
0,2	92	92	56	52
0,4	95	93	60	54
0,8	98	95	68	58

 $\Delta^{(1)}$ is approximately proportional to q, so that (except when ζ and θ are both large) the rules mentioned above become even more pronounced as q increases; eventually, for large q, the role of $I_q^{(1)}$ becomes minor and the behavior of $I_q^{(1)}$ follows that of $\Delta^{(1)}$ alone.

Let us now consider some numerical examples. Table 1 contains $100 \ \frac{I_q^{(1)}\left(0,\ \theta,\ \psi\right)}{I_q^{(1)}\left(\tau^*,\theta,\psi\right)} \ \text{for} \ \tau \ * = 0.2 \ \text{and} \ 0.6, \ \text{showing how} \ I_q^{(1)} \ \text{varies with} \ \tau \, .$

Table 2 contains the quantity $100 \ \frac{\left[I_q^{(1)}\left(\tau^*,\,\theta,\,\psi\right)\right]_{\theta=0^\circ}}{\left[I_q^{(1)}\left(\tau^*,\,\theta,\,\psi\right)\right]_{\theta=75^\circ}}$, showing how $I_q^{(1)}$ varies with θ .

Table 3 contains the quantity 100 $\frac{\left[I_q^{(1)}\left(\tau^*,\theta,\;\psi\right)\right]_{\zeta=75^{\circ}}}{\left[I_q^{(1)}\left(\tau^*,\theta,\;\psi\right)\right]_{\zeta=30^{\circ}}}\,,\;\text{showing how }I_q^{(1)}\;\text{varies with }\zeta\;.$

TABLE 6

		$\zeta = 30^{\circ}$		ζ=75°		
τ*	$\theta = 0^{\circ};$ $\psi = 0^{\circ}$	$ \theta = 75^{\circ}; $ $ \psi = 0^{\circ} $	$\theta = 75^{\circ} \\ \psi = 180^{\circ}$	$\theta = 0^{\circ};$	$ \theta = 75^{\circ}; $ $ \psi = 0^{\circ} $	$\theta = 75^{\circ};$ $\psi = 180^{\circ}$
0,2	16	5,5 3.0	6,2 $3,2$	7,0	1,5 1,2	$\frac{2}{1}, \frac{2}{4}$

TABLE 7

	<i>q</i> =	=0	<i>q</i> =	=0,2	q=	0,4	<i>q</i> =	0.8
τ	0=0°	0 == 60°	θ === 0.0	θ =60°	0=00	θ == 60°	θ=00	0=60
				$\tau^* = 0, 2$				
(),()()	0,00	0,00	0,33	0,33	0,67	0,67	1,41	1,41
0,050	0,02	0,03	0,34	0,34	0,68	0,68	1,41	1,39
0,100	0,04	0,05	0,35	0,35	0,69	0,68	1,41	1,37
0,125	0,04	0,06	0,36	0,36	0,69	0,68	1,41	1,36
0,450	0,05	0,07	0,37	0,37	0,70	0,68	1,41	1,35
0,160	0,06	0,08	0,37	0,37	0,70	0,68	1,41	1,35
0,170	0,06	0,08	0,38	0,38	0,70	0,68	1.41	1,34
0,180	0,07	0,09	0,38	0,38	0,70	0,68	1,41	1,33
0,190	0,08	0,10	0,38	0,38	0,71	0,69	1,41	1,33
0,200	0,08	0,10	0,39	0,39	0,71	0,69	1,41	1,33
				$\tau^* = 0.6$				
(),()()	0,0	0,0	0,30	0,30	0,64	0,64	1,46	1,46
0,10	0,02	0,05	0,32	0,34	0,66	0,67	1,46	1,45
0,20	0,04	0,09	0,34	0,37	0,67	0,68	1,46	1,43
0,30	0,06	0,13	0,35	0,40	0,67	0,69	1,45	1,41
0,40	0,08	0,16	0,36	0,41	0,68	0,69	1,45	1,39
0,45	0,09	0,17	0,37	0,41	0,68	0,69	1,43	1,34
0,50	0,12	0,20	0,39	0,43	0,69	0,70	1,43	1,32
0,55	0,44	0,23	0,41	0,45	0,71	0,70	1,42	1,30
0,57	0,15	0,24	0,42	0,45	0,71	0,70	1,42	1,29
0,58	0,16	0,25	0,42	0,46	0,71	0,70	1,42	1,28
0,59	0,16	0,25	0,43	0,46	0,71	0,70	1,42	1,28
0,60	0,17	0,25	0,43	0,46	0,72	0,70	1,41	1,28

Table 4 contains the quantity 100 $\frac{\left[I_q^{(1)}(\tau^*,\theta,\psi)\right]_{\tau^*=0,2}}{\left[I_q^{(1)}(\tau^*,\theta,\psi)\right]_{\tau^*=0,6}}, \text{ showing how } I_q^{(1)}(\tau^*,r)$ varies with increasing τ^* .

Table 5 gives the ratio 100 $\frac{\left[I_q^{(1)}(\tau^*,\theta,\psi)\right]_{\theta=75^\circ,\,\psi=180^\circ}}{\left[I_q^{(1)}(\tau^*,\theta,\psi)\right]_{\theta=75^\circ,\,\psi=0^\circ}}, \text{ which characterizes}$ the azimuthal variation.

Finally, Table 6 contains the ratio $\frac{\left[I_q^{(1)}\right]_{q=0,8}}{\left[I_q^{(1)}\right]_{q=0}}$, showing how $I_{\mathbf{q}}^{\mathbf{(1)}}$ increases with q.

Tables 1-6 illustrate the manner in which $I_q^{(1)}$ varies, as described above, and enable us to state the following.